NANO LETTERS

pubs.acs.org/NanoLett

Directional Photofluidization Lithography for Nanoarchitectures with Controlled Shapes and Sizes

Seungwoo Lee,[†] Jonghwa Shin,[‡] Yong-Hee Lee,[‡,§] Shanhui Fan,[⊥] and Jung-Ki Park*[,†,§,∥]

[†]Department of Chemical and Biomolecular Engineering, [‡]Department of Physics, [§]KAIST Institute for the Nanocentury, [∥]KAIST Graduate School of EEWS, Korea Advanced Institute of Science and Technology (KAIST), 335 Gwahangno, Yuseong-gu, Daejeon 305-701, Republic of Korea, and [⊥]E. L. Ginzton Lab and Department of Electrical Engineering, Stanford University, Stanford, California 94305

ABSTRACT Highly ordered metallic nanostructures have attracted an increasing interest in nanoscale electronics, photonics, and spectroscopic imaging. However, methods typically used for fabricating metallic nanostructures, such as direct writing and template-based nanolithography, have low throughput and are, moreover, limited to specific fabricated shapes such as holes, lines, and prisms, respectively. Herein, we demonstrate directional photofluidization lithography (DPL) as a new method to address the aforementioned problems of current nanolithography. The key idea of DPL is the use of photoreconfigurable polymer arrays to be molded in metallic nanostructures instead of conventional colloids or cross-linked polymer arrays. The photoreconfiguration of polymers by directional photofluidization allows unprecedented control over the sizes and shapes of metallic nanostructures. Besides the capability for precise control of structural features, DPL ensures scalable, parallel, and cost-effective processing, highly compatible with high-throughput fabrication. Therefore, DPL can expand not only the potential for specific metallic nanostructure applications but also large-scale innovative nanolithography.

KEYWORDS Surface plasmon resonance, metallic nanostructures, azopolymer, directional photofluidization

Plasmonics is the study of the optically active collective oscillations of conduction electrons in metallic nanostructures; such electron oscillations can provide an efficient way for the localization and enhancement of the electromagnetic field (light) below the diffraction limit.[1−4] The phenomenon of electron oscillations is of dramatic technological importance for nanophotonics,[5−10] nanospectroscopic imaging,[11−13] and energy devices.[14,15] Recently, various metallic nanostructures including nanobowties,[16] nanorods,[7,8,17] nanopyramids,[18] nanorices,[19] nanocrescents,[20] and nanograils[21] have been proposed to efficiently localize the electromagnetic field below the diffraction limit by various research groups. In particular, metallic nanostructures with sharp edges, for example, the tips of the wings of nanobowties,[22] have attracted research interest, as the sharp edges exhibit a much higher localized electromagnetic field, compared to rounded edges.[23,24]

To date, these metallic nanostructures have been fabricated predominantly by two different approaches: (i) direct writing-based methods and (ii) template-based pattern transfer methods. Direct-writing-based methods such as focused ion beam (FIB) lithography,[25] electron beam lithography,[26] and multiphoton lithography[27] have enabled the fabrication of metallic nanostructures with finely tuned structural features including the sizes, gaps, and shapes associated with these types of nanostructures. However, the impractically low throughput of the serial direct-writing process is a major obstacle to the large-area fabrication of metallic nanostructures. Metal transfer through a nanotemplate which can be simply developed via nanosphere lithography (NSL),[28,29] interference lithography (IL),[30] and soft lithography (SL),[31,32] have advantages, especially on account of the ability to fabricate large-area metallic nanostructures in parallel, in contrast to direct-writing-based methods: monolayered colloidal arrays (NSL), photoresist post arrays (IL), and PDMS arrays (SL) can be used as a robust and useful template for pattern transfers by selective metal evaporation and a subsequent lift-off process. However, despite their usefulness, these techniques are limited to the fabrication of specific shapes (for example, holes, lines, and prisms). Recently, Whitesides et al. successfully fabricated various metallic nanostructures such as nanorings, nanowires, and curved nanorods by transferring epoxy slab possessing patterned metallic structures to the substrate (Nanoskiving). However, the process involved, for instance, the sectioning of epoxy films with an ultramicrotome, is quite complicated and challenging. Moreover, this process is not conveniently available to general users.[33−35]

Herein, we present a simpler method, termed "directional photofluidization lithography" (DPL), as a new approach to address the aforementioned limitations. The key idea of DPL

* To whom correspondence should be addressed. E-mail: jungpark@kaist.ac.kr. Website: zoo.kaist.ac.kr; web.kaist.ac.kr/~ace51. Tel: +82-42-350-3925. Fax: +82-42-350-3910 .

Received for review: 10/25/2009
Published on Web: 12/17/2009

DOI: 10.1021/nl903570c | *Nano Lett.* **2010,** *10,* 296-304

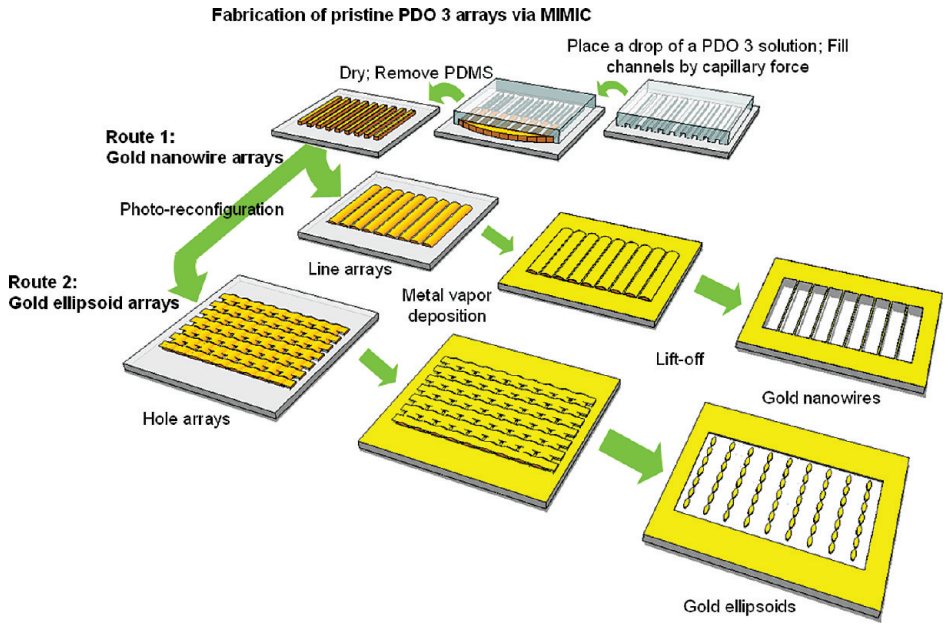

FIGURE 1. Schematic illustration of directional photofluidization lithography (DPL): DPL consists of three main steps: (i) generation of pristine photoreconfigurable polymer templates (PDO 3) by micromolding in capillaries (MIMIC) with solvent; (ii) the photoreconfiguration of PDO 3 line arrays by controlled light irradiation (single-beam irradiation and holographic interference pattern irradiation); (iii) gold deposition and subsequent removal of templates by a lift-off process (rinsing with solvent).

is to use photoreconfigurable polymer arrays as a template to mold metals instead of a conventional colloidal nanosphere, photoresist arrays, and PDMS arrays. In this method, the optical manipulation of polymer arrays by varying the polarization and irradiation time allows unprecedented control of the structural features, including the shapes and sizes. It also enables the creation of a sharp edge. Furthermore, the overall procedures of DPL ensure scalable, parallel, and low-cost processing. Consequently, the photoreconfiguration of a polymer template in combination with the thin film deposition of metals enables high-throughput and large-area fabrication of metallic nanostructures with precisely tuned structural features. Below, we describe the fabrication of large-area metallic nanostructures (square millimeters) of gold nanowire and ellipsoid arrays by means of DPL to demonstrate its versatility as a nanolithographic technique. The optical properties of gold ellipsoid arrays are also characterized and analyzed.

The photoreconfiguration of polymer templates, the key patterning step in DPL, is based on the directional photofluidization of azobenzene-containing polymer (abbreviated as azopolymer) in which azobenzene molecules are covalently attached to a polymeric main chain. Specifically, an azopolymer thin film can behave as a fluid under light irradiation, and the direction of their fluidity strongly depends on the light polarization. Additionally, the photofluidization distance of an azopolymer can be controlled simply by adjusting the light irradiation time. More importantly, the irradiation of a spatially arranged light pattern, for example, a light interference pattern, enables local manipulation of the photofluidization of azopolymer templates, with allows the fabrication of metallic particles with sharp edges and the efficient localization of the electromagnetic field.[23,24] Therefore, this directional photofluidization allows us precise manipulation of the movement and resulting shapes of polymer templates to be molded in metallic arrays by varying the light irradiation conditions of the light polarization, irradiation time, and geometries of the light pattern.

By way of demonstration, we fabricated both gold nanowire (route 1) and ellipsoidal particle arrays (route 2) by DPL, as described in Figure 1. The DPL procedure consists of three principal steps: (i) generation of pristine photoreconfigurable polymer templates with rectangular lines by micromolding in capillaries (MIMIC) with solvent; (ii) photoreconfiguration of the polymer templates by controlled light irradiation (single beam irradiation or holographic interference pattern irradiation); (iii) gold deposition and the subsequent removal of the templates by a lift-off process. Epoxy-based poly(disperse orange 3), abbreviated as PDO 3, was used as a linear azopolymer to be molded in the capillaries: the details of PDO 3 are described in Figure S1 in the Supporting Information. Details of MIMIC with the solvent[36,37] are also described in Figures S2−5 in the Supporting Information.

Figure 2a displays the obtained pristine PDO 3 line arrays: the low-magnification optical microscopic (OM) image clearly shows the moiré fringes due to the uniformity of the PDO 3 lines over a large area (~1.8 mm^2) (see Figure S6 in the Supporting Information); in the inset of Figure S6 in the Supporting Information, Fourier transform (FT) of the corresponding OM image further confirms the long-range order within PDO 3 line arrays. The width and periodicity of the resulting PDO 3 lines were 1.30 and 3.84 μm, respectively.

DOI: 10.1021/nl903570c | *Nano Lett.* **2010,** *10,* 296-304

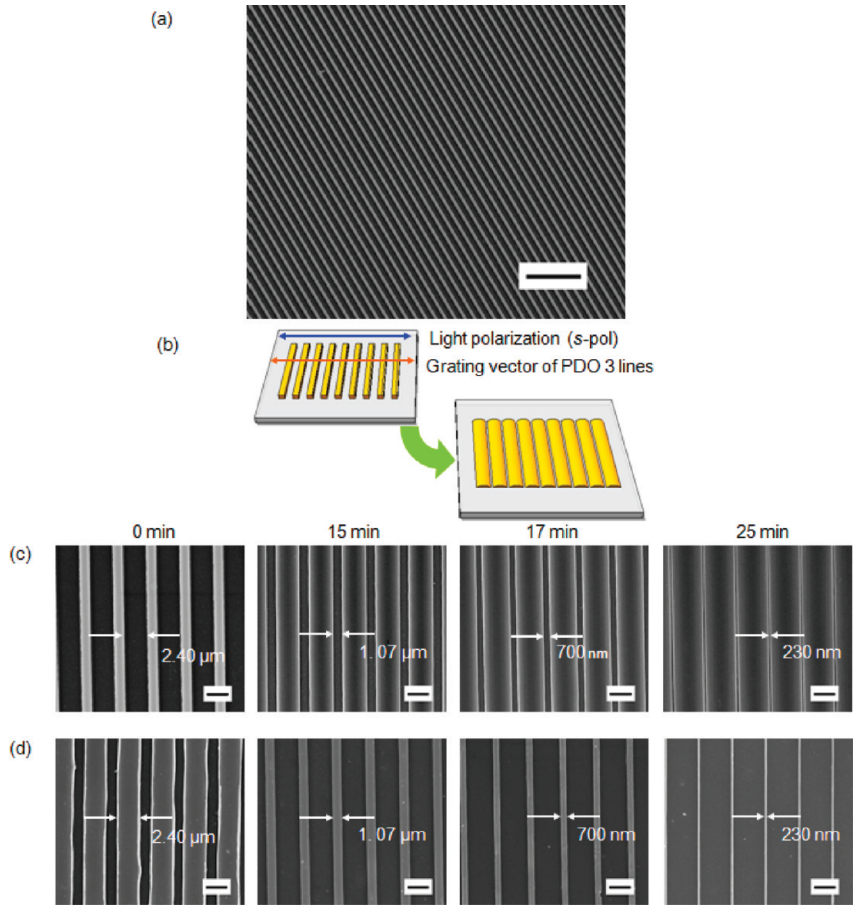

FIGURE 2. Photoreconfiguration of polymer templates by single-beam irradiation and pattern transfer: (a) SEM image of PDO 3 line arrays fabricated by MIMIC with NMP. (b) Schematic illustration of the process. (c) SEM images of photoreconfigured PDO 3 line arrays versus the irradiation time. (d) SEM images of gold nanowire arrays versus the irradiation time. The width of the gold nanowire was reduced by at least a factor of 1040%. The roughness of the pattern (line-edge roughness) was reduced by a factor of 475% (defined as the ratio of the initial roughness to the final roughness) after photofluidization. Scale bars are (a) 25 μm and (c, d) 2.5 μm.

The thickness of PDO 3 line was 1.3 μm. We illuminated PDO 3 line arrays with an s-polarized, spatially filtered, single beam from a laser light source (488 nm, 35.5 mW/cm^2, Melles Girot) (see Figure S7 in Supporting Information): the electric vector of the s-polarization is parallel to the grating vector of a PDO 3 rectangular line pattern as shown in Figure 2b. Figure 2c shows scanning electron microscopy (SEM) images of photoreconfigured PDO 3 lines as a function of the irradiation time. Indeed, the spacing between the two PDO 3 lines (the trench width of the PDO 3 lines) was reduced with the light irradiation time as a result of the directional photofluidization along the light polarization: the initial 2.45 μm spacing became ~230 nm after light irradiation of 25 min. On the other hand, interestingly, the irradiation of light with a polarization perpendicular to the grating vector of PDO 3 line arrays (p-polarization) did not give rise to photofluidization as shown in Figure S8 in the Supporting Information.

The fluidic behavior of azopolymer under light irradiation has attracted considerable interest since the phenomenological finding of surface relief gratings (SRGs): the SRGs were spontaneously generated by the irradiation of interferential light pattern onto the azopolymer thin film, and the photoisomerization of azobenzene and the resulting polymer migration are though to be closely related to the formation of SRGs.[38−40] In addition to the SRGs, Hubert et al. observed the formation of two-dimensional hexagons, when one beam is imaged onto the azopolymer thin film.[41] It should be noted that these photofluidization-induced formations of surface reliefs showed the structural dependence on the light polarization: the polarization of incident light considerably influences on the degree of polymer migration and the orientation of hexagons (parallel to the light polarization).[38−41] These observations of polarization-dependent photofluidization of azopolymer thin film indicate that the photofluidity of azopolymer is closely related to the photoisomerization of azobenzene molecules and the resulting anisotropic alignment in the direction perpendicular to the light polarization. Hence, their anisotropic alignment likely gives rise to anisotropic photoinduced motion as well as anisotropic stress and anisotropic intermolecular interaction.[41] Indeed, to rationalize this anisotropic photofluidization of azopolymer, Juan et

DOI: 10.1021/nl903570c | *Nano Lett.* **2010,** *10,* 296-304

al. developed a statistical model based on the interaction between fundamental molecular dipole and light and successfully predicted the various polarization-dependent photofluidization phenomena.[42] Our results of the polarization-selective photoreconfiguration of the azopolymer lines further support the assumption that the directional photofluidization of azopolymer is responsible to a large extent for the photoinduced anisotropic alignment of azobenzene molecules with respect to the light polarization and the resulting anisotropic motion. However, the underlying mechanisms of the direction photofluidization of azopolymer have to be further investigated for the better understanding.

Photoreconfigured PDO 3 line arrays by directional photofluidization can act as a nanotemplate to mold metallic nanowire arrays. To demonstrate this, a chromium adhesion layer (4 nm) and a gold layer (40 nm) were evaporated over PDO 3 line arrays on a quartz substrate via e-beam evaporation, and the PDO 3 templates were then removed by a mild lift-off process. This process was carried out by rinsing with acetone for 2 min and with NMP for 5 min in an ultrasonic bath. As the glass transition temperature of PDO 3 is relatively high (~120 °C), the photoreconfigured organic template maintained its structural integrity during e-beam evaporation even under high process temperature. Figure 2d shows SEM images of the obtained gold nanowire arrays with a controlled width. Given that they consist of a linear polymer with relatively low molecular weight (~4700, as described in the Supporting Information), PDO 3 line arrays can be completely removed by a simple solvent treatment, as is evidenced from the lack of a structure-guiding PDO 3 pattern. The low adhesion properties of PDO 3 also can trigger the removal of polymer template from the substrate (quartz) without residue. The widths of the gold nanowires were actually reduced as the spacing between the PDO 3 lines decreased: the initial 2.45 μm width was reduced to 230 nm. The corresponding width of the gold nanowire was commensurate with the spacing of the photoreconfigured PDO 3 lines, and the total reducing factor was 1040%. The use of modified soft-lithographic techniques including mechanical compression, bending, and stretching also can reduce the structural features efficiently, but the use of mechanically modified PDMS for nanolithography suffers from some problems associated with the sagging to the PDMS mold during the mechanical contact with substrate, especially in the high-resolution fabrication.[43] On the contrary, DPL has advantages over the soft-lithographic techniques on account of its unique ability to manipulate the sizes of template by the remote irradiation of optical field, and thus free from any problems that could be caused by the mechanical contact. As a result, the photoreconfiguration of a polymer template through directional photofluidization allows unprecedented control of the dimensionalities of nanowire even under high-resolution fabrication, which is critical for numerous applications of nanolithography. Moreover, the gold nanowire arrays from the photoreconfigured

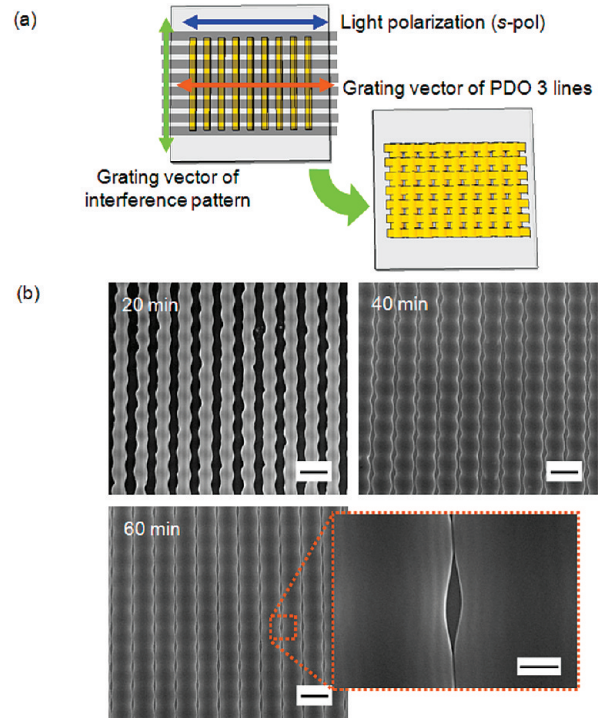

FIGURE 3. Photoreconfiguration of PDO 3 line arrays by irradiation of an interferential pattern: (a) Schematic illustrations of the process. (b) SEM images of photoreconfigured PDO 3 line arrays (hole arrays) versus the irradiation time. The unique characteristic sinusoidal intensity profile of the interference light pattern leads to the formation of a hole with a stream line which is similar in appearance to an ellipsoid or a grain of rice. Scale bars are 5 μm (magnification SEM of 60 min, 1 μm).

template showed a smooth edge line, as a result of the uniform photofluidization of the PDO 3 lines and the minimization of the surface energy, whereas rough line edges were clearly observed in gold nanowire arrays derived from a pristine PDO 3 pattern: the initial line-edge roughness was reduced from 19 to 4 nm (a factor of 475%). From these results of replications with high fidelity and reduced line-edge roughness, we can establish that azopolymer can serve as a useful nanotemplate for pattern transfers; thus, DPL offers a very efficient fabrication method for nanowire arrays with tunable dimensions that are essential for a wide range of potential applications to photonic and electronic nanodevices.[44,45]

To verify the versatility of DPL further, the hole arrays in PDO 3 thin film were created by the localized directional photofluidization of PDO 3 line arrays. In particular, the localized directional photofluidization in this work was induced by the irradiation of an interference light pattern. In the interference pattern, the intensity of the light is spatially modulated along the grating vectors of the interference pattern;[40] consequently, the irradiation of the interference pattern onto the azopolymer could give rise to directional photofluidization selectively only in the bright regions of the interference pattern. The use of an interference

DOI: 10.1021/nl903570c | *Nano Lett.* **2010,** *10,* 296-304

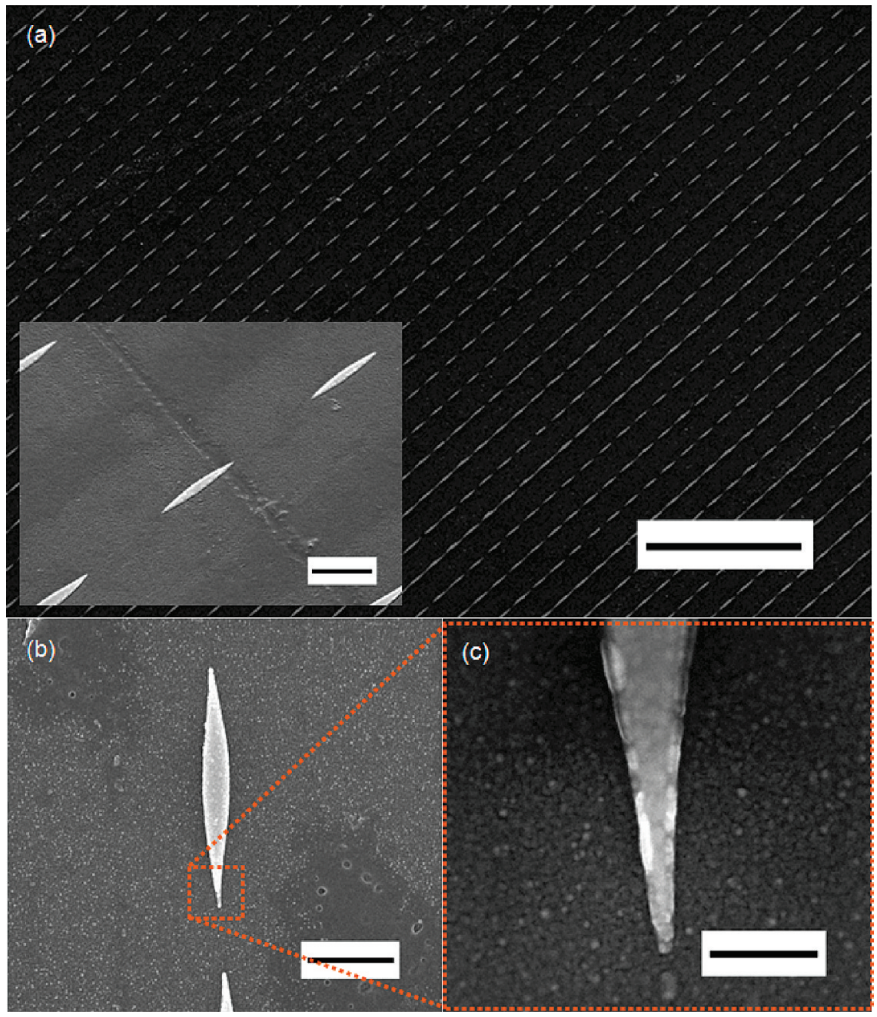

FIGURE 4. SEM images of gold ellipsoids: (a) Gold ellipsoids arranged over a large area with structural uniformity. (b) High-magnification SEM image of a single gold ellipsoid. (c) Tips of a single gold ellipsoid. The radii of curvature are less than 25 nm (from 12 to 25 nm). Scale bars are (a) 20 μm (inset, 1 μm), (b) 1 μm, and (c) 250 nm.

pattern has several advantages over conventional photon-irradiation through a mask: (i) the process steps for the alignment of the photomask can be greatly simplified, because the irradiation of the interfered beams enables maskless patterning; (ii) the dimensionalities and geometries of the interference pattern can be precisely controlled through a simple adjustment of the beam parameters of the incident angle, polarization, and the number of beams to be mixed together; (iii) localized directional photofluidization can occur periodically, allowing the fabricated holes in the PDO 3 film to be arranged over a large area. In this work, we used a one-dimensional (1D) interference light pattern that was generated by interfering the two beams with s-polarization, parallel to the gratings vectors of the PDO 3 line arrays (see Figure 3a). The employed incident angle and intensity of the beam were 4° and 30.0 mW/cm^2, respectively. The calculated period of the interference pattern with Bragg's condition was 3.49 μm. Here, the grating vector of the interference pattern should be placed in a direction perpendicular to that of the PDO 3 line arrays to induce the local photofluidization of the azopolymer, as described in Figure 3a. Figure 3b shows the irradiation time evolution of locally photoreconfigured PDO 3 templates. At the initial stage of interference pattern irradiation (~20 min), continuous PDO 3 lines with a dumbbell-like shape were clearly observed. This results from the lateral protrusions (or directional creeping) of the PDO 3 lines according to the bright regions of the interference pattern; this selective and directional photofluidization also occurred only along the light polarization, precisely as in a one-beam irradiation process. The corresponding period of localized photofluidization (localized lateral protrusions) was well-matched with Bragg's condition. When the irradiation time increased from 20 to 60 min, a pair of protruding regions along the grating vectors of the PDO 3 line arrays (marked by the orange dotted line in Figure 3b) was found to have merged, due to the continuing directional photofluidization. Accordingly, the spacing between the PDO 3 lines in the bright regions of the

DOI: 10.1021/nl903570c | *Nano Lett.* **2010,** *10,* 296-304

interference pattern was eventually unobservable; instead, holes arranged regularly over a broad area were produced, as shown in Figure 3b. Interestingly, we observed that the holes produced were ellipsoidal with sharp edges rather than circular. The formation of these holes with a stream line is attributable to the unique characteristic sinusoidal intensity profile of the interference light pattern, unlike the intensity profile developed by photon irradiation through the photomask (see Figure S9 in Supporting Information). This gradient photofluidization along the grating vector of the interference pattern indicates that the degree of photofluidization is also determined by the light intensity as well as by the irradiation time; consequently, a sinusoidal protrusion of the azopolymer occurs. Hence, localized directional photofluidization using an interference pattern offers additional flexibility in conjunction with the advantages of fabricating regularly arranged hole arrays and controlling their shapes toward an efficient localizing electromagnetic field.

Using the same pattern transfer process as described in the previous section involving the fabrication of gold nanowires, we successfully transferred the obtained hole arrays into free-standing gold ellipsoid arrays. The SEM image of the gold ellipsoid arrays in Figure 4a shows that the individual gold ellipsoids are highly ordered over a large area with few defects and structural variation (the structural variation was less than 25 nm). These observations confirm that DPL enables the production of large-area metallic nanostructures with controlled shapes and structural homogeneity. The structural features of the obtained gold ellipsoids including the length (x, the long axis of the gold ellipsoid), width (y, the short axis of the gold ellipsoid), period, and gaps between the sharp edges were commensurate with those of the photoreconfigured PDO 3 pattern. We also found that a magnified image of single gold ellipsoid (inset in Figure 4a) reveals a smooth surface morphology and low line-edge roughness (below 5 nm). More significantly, it should be pointed out that the radii of curvature of the edge at the end of the ellipsoid ranged from 12 to 25 nm (see Figure 4b,c): contrary to the gold nanowires, some types of residue were observed near a gold ellipsoid, possibly due to the trace of solvent evaporation. These obtained values of radii of curvatures are comparable to that done by e-beam lithography or FIB. The nanoscale tips of these ellipsoids can concentrate the electromagnetic fields efficiently; thus, this gold ellipsoid with its sharp edges can be used as an optical antenna[7,8] and as a nanostructure for SERS.[11,12]

In the nanolithography, the ability to tune the pattern dimensions is of practical significance for numerous applications. The dimensions (x, y) of the gold ellipsoid can be precisely controlled by adjusting the irradiation time, as can the gold nanowires. Figure 5 demonstrates the influence of the irradiation time of the interference pattern on the dimensions of the gold ellipsoid. Indeed, both the length (x) and width (y) were simultaneously reduced as the irradiation time increased, while the y/x ratios were almost maintained:

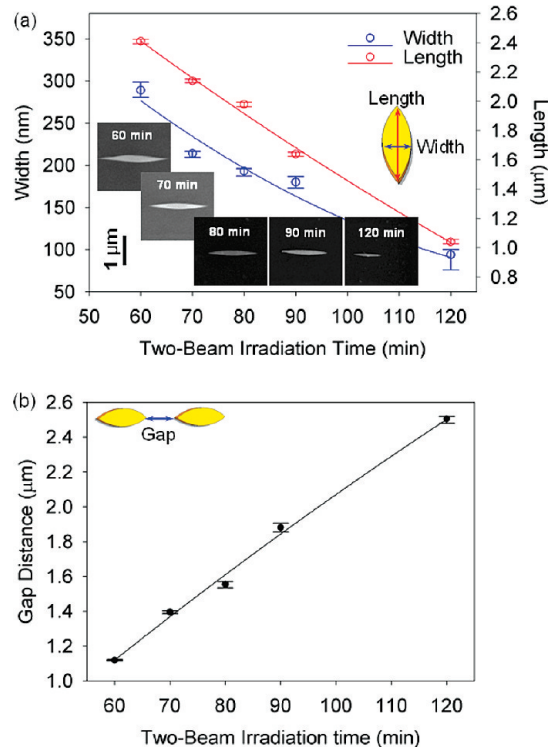

FIGURE 5. Tunability of structural dimensions by varying the two-beam irradiation time: (a) Plot of the structural dimensions and SEM images of a gold ellipsoid versus the irradiation time. (b) Plot of gap distances versus the irradiation time. Both the length (x) and the width (y) of the gold ellipsoid were simultaneously reduced with the irradiation time, while the y/x ratios remained almost unchanged (from 0.08 to 0.10).

it ranged from 0.08 to 0.10. The gaps between the sharp edges were increased as a result of the reduced length of the ellipsoid. Furthermore, the radii of curvature of the tips remained nearly unchanged, even under a structural reduction (variability in radii of curvature ranged from 12 to 25 nm across the samples). A common drawback of the control of dimensions by varying the irradiation time of the interference pattern, however, is the inability to tune the length (x) or width (y), independently. The control of other process parameters such as the incident angle of the beams and the light intensity would address this problem, thereby providing further flexibility to tune the dimensions of gold ellipsoids.

Finally, to investigate the optical response of gold ellipsoids, the amount of optical scattering was measured using an optical microscope with dark-field illumination (visible to near-infrared) and Fourier-transform infrared spectroscopy combined with a microscope (infrared). The details of the experimental setup and optical characterizations are described in Figures S10−11 in the Supporting Information. Panels a and b of Figure 6 show the far-field optical scattering spectra of gold ellipsoids with different dimensions controlled by varying the light irradiation time and light polarization. In general, such rodlike metallic nanostructures exhibit significant reflectance at the wavelength position where surface plasmon resonance occurs,

DOI: 10.1021/nl903570c | *Nano Lett.* **2010,** *10,* 296-304

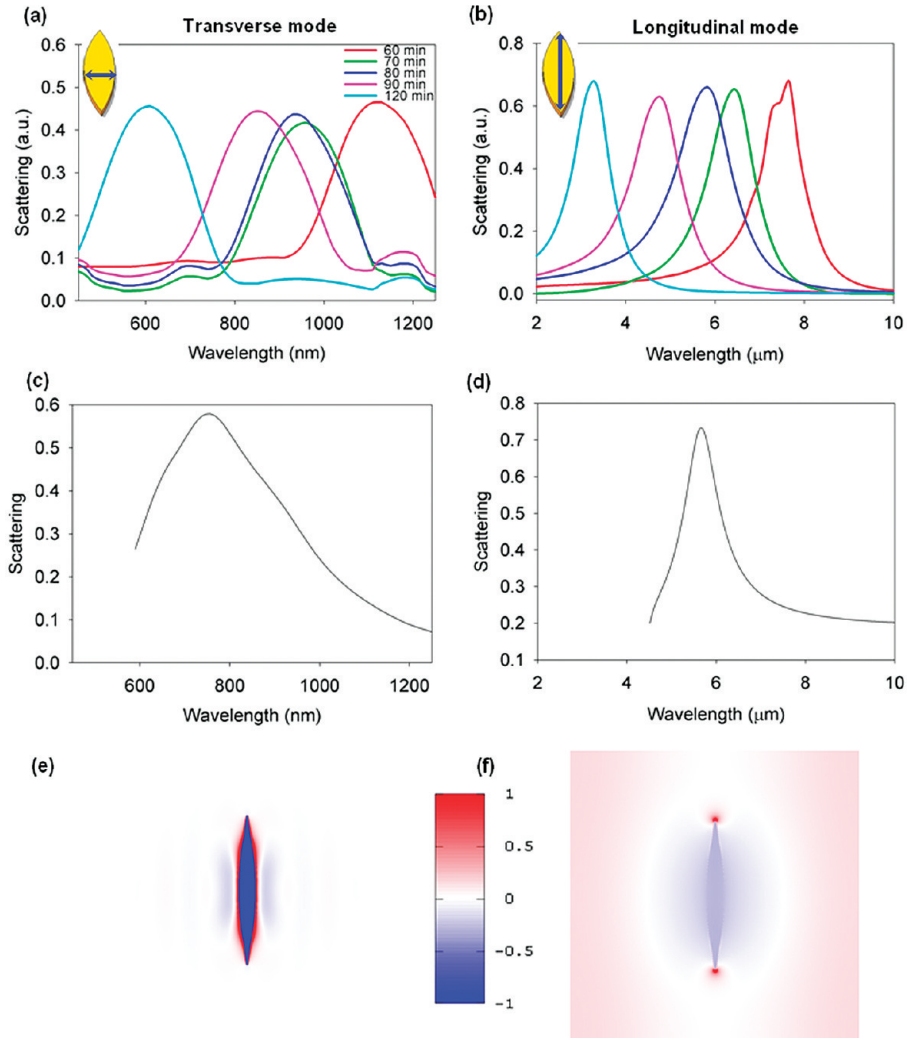

FIGURE 6. Optical properties of gold ellipsoids: (a, b) Dependence of the scattering resonance as a function of the dimensions of the gold ellipsoid. (c, d) Calculated far-field scattering spectra. (e, f) Near-field profile under resonance excitations. The left and right panels indicate the transverse and longitudinal modes, respectively.

and their optical responses strongly depend on the dimensions of the structures and the light polarization. The strong resonance features are clearly visible in the scattering spectra, i.e., from 600 to 1075 nm (Figure 6a, transverse mode) and from 2.8 to 7.4 μm (Figure 6b, longitudinal mode), showing the trend in the red shift of the maxima as the size of the gold ellipsoids increases: a shoulder observed around 8 μm for the longitudinal mode can be attributed to the structural variation caused by the inherent nature of the fabrication process (for example, noise in the photon or scattering). Furthermore, the scattering peaks corresponding to the longitudinal polarization are sharper and more pronounced as compared to the transverse mode, possibly due to lower optical loss of gold at longer wavelengths as well as the highly anisotropic shape of the resonator. Meanwhile, in both the transverse and longitudinal modes, there are no significant variations in the scattering for the samples with different dimensions. Interestingly, we also observed the peaks around 1200 nm. At this stage, the nature of the peaks near 1200 nm is not clearly understood. However, it is likely that these peaks are not related to the surface plasmon at least, as evidenced from independence of the peaks on the dimension of structures. We conjecture that the peaks near 1200 nm can be originated from the diffraction due to the periodicity of the arrays, but their underlying mechanism of these peaks has to be studied in more detail. To confirm that these strong scattering features (from 600 to 1075 nm and from 2.8 to 7.4 μm) are indeed coupled to the surface plasmon resonances, a numerical analysis the surface plasmon resonances was conducted using a finite-difference time-domain (FDTD) method with Yee's discretization scheme.[46,47] The lateral sizes of the computational domain were chosen to be equal to the periods of the fabricated sample (two beam irradiation for 90 min), and a periodic boundary condition was adopted (further details are described in Figure S12 in the Supporting Information).[46] Perfectly matched layers terminate the domain in the vertical direction at 2 μm.[48] The computational domain is dis-

DOI: 10.1021/nl903570c | *Nano Lett.* **2010,** *10,* 296-304

cretized in 2−4 nm steps. Mirror symmetries are exploited to reduce the computation by 2- or 4-fold when possible. The FDTD analysis of far-field optical scattering spectra of the gold ellipsoids is shown in panels c and d of Figure 6. The simulation results showed resonance features similar to the experimentally measured optical scattering. The slight differences in the resonance position and sharper peaks compared to the experimental measurement can be explained by the structural variation and the factors neglected in the FDTD simulation. From the near-field profiles of the gold ellipsoids (Figure 6, panels e and f), we confirm that the resonance peaks described in Figure 6a and 6b correspond to the transverse and longitudinal surface plasmons of gold ellipsoids, respectively.

In conclusion, this work is based on the use of a photoreconfigurable template as a novel strategy for the patterning of nanoarchitectures. By taking advantage of the directional photofluidity of azopolymer, DPL allows nanotemplate shape/size to be precisely controlled. It is therefore anticipated that the newly proposed method will provide an efficient route to well-registered nanoarchitectures. As proof of its versatility as a nanolithographic technique, we fabricated gold nanowire and ellipsoid arrays. In particular, the sinusoidal intensity profile gave rise to the formation of a hole with a streamline, which is very difficult to fabricate with other lithographic techniques. Moreover, as the photoreconfigurable template can be easily removed by a mild cleaning process, most metallic nanostructures, replicating a photoconfigured polymer pattern with controlled shape/size, can be transferred onto a substrate with high structural fidelity. More importantly, DPL also can be applied to the other types of polymer templates for a nanolithography as well as line arrays used in this study. Especially, the colloid arrays with photofluidity can expand the potential of colloidal or nanosphere lithography in terms of the control of colloidal shapes and resulting transferred nanoarchitectures by a simple light irradiation. This work is underway in our research group and will be reported in a forthcoming paper. Upon these points of view, it represents very important progress toward the development of more advanced nanolithographic techniques. We believe that DPL offers a very significant opportunity for the fabrication of novel nanostructure arrays and their potential application to nanodevices.

Acknowledgment. This publication was based on work supported by a grant (code#: 09K1501-02510) from the "Center for Nanostructured Materials Technology" under the "21st Century Frontier R&D Programs" of the Ministry of Education, Science, and Technology, Korea. This work was also supported by a grant from the Brain Korea 21 Program. One of the authors, S.L., would like to thank the Korea Science and Engineering Foundation for financial support (code# S2-2008-000-01855-1). S.L. would also like to thank Dr. J. Lee of Dongwoo Optron Co., Ltd., for his valuable assistance and discussions.

Supporting Information Available. Experimental details and supporting results are described. This material is available free of charge via the Internet at http://pubs.acs.org.

REFERENCES AND NOTES

(1) Kreibig, U.; Vollmer, M. *Optical Properties of Metal Clusters*; Springer-Verlag: Berlin, Germany, 1995.
(2) Barnes, W. L.; Dereux, A.; Ebbesen, T. W. *Nature* **2003**, *424*, 824.
(3) Maier, S. A.; Atwater, H. A. *J. Appl. Phys.* **2005**, *98*, No. 011101/1.
(4) Murray, W. A.; Barnes, W. L. *Adv. Mater.* **2007**, *19*, 3771.
(5) Engheta, N. *Science* **2007**, *317*, 1698.
(6) Akimov, A. V.; Mukherjee, A.; Yu, C. L.; Chang, D. E.; Zibrov, A. S.; Hemmer, P. R.; Park, H.; Lukin, M. D. *Nature* **2007**, *450*, 402.
(7) Crozier, K. B.; Sundaramurthy, A.; Kino, G. S.; Quate, C. F. *J. Appl. Phys.* **2003**, *94*, 4632.
(8) Mühlschlegel, P.; Eisler, H.-J.; Martin, O. J. F.; Hecht, B.; Pohl, D. W. *Science* **2005**, *208*, 1607.
(9) Smith, D. R.; Pendry, J. B.; Wiltshire, M. C. K. *Science* **2004**, *305*, 788.
(10) Shalaev, V. M. *Nat. Photonics* **2007**, *1*, 41.
(11) Nie, S.; Emory, S. R. *Science* **1997**, *275*, 1102.
(12) Haynes, C. L.; Van Duyne, R. P. *J. Phys. Chem. B* **2003**, *107*, 7426.
(13) Zhang, X.; Liu, Z. *Nat. Mater.* **2008**, *7*, 435.
(14) Catchpole, K. R.; Polman, A. *Opt. Express* **2008**, *16*, 21793.
(15) Ferry, V. E.; Sweatlock, L. A.; Pacifici, D.; Atwater, H. A. *Nano Lett.* **2008**, *8*, 4391.
(16) Fromm, D. P.; Sundaramurthy, A.; Schuck, P. J.; Kino, G.; Moerner, W. E. *Nano Lett.* **2004**, *4*, 957.
(17) Thomas, K. G.; Barazzouk, S.; Ipe, B. I.; Joseph, S. T. S.; Kamat, P. V. *J. Phys. Chem. B* **2004**, *108*, 13066.
(18) Lee, J.; Hasan, W.; Lee, M. H.; Odom, T. W. *Adv. Mater.* **2007**, *19*, 4387.
(19) Wang, H.; Brandl, D. W.; Le, F.; Nordlander, P.; Halas, N. J. *Nano Lett.* **2006**, *6*, 827.
(20) Wu, L. Y.; Ross, B. M.; Lee, L. P. *Nano Lett.* **2009**, *9*, 1956.
(21) Heo, C.-J.; Kim, S.-H.; Jang, S. G.; Lee, S. Y.; Yang, S.-M. *Adv. Mater.* **2009**, *21*, 1726.
(22) Sundaramurthy, A.; James Schuck, P.; Conley, N. R.; Fromm, D. P.; Kino, G. S.; Moerner, W. E. *Nano Lett.* **2006**, *6*, 355.
(23) Novotny, L.; Bian, R. X.; Xie, X. S.; Leung, P. T. *Phys. Rev. Lett.* **1997**, *79*, 645.
(24) Kelly, K. L.; Coronado, E.; Zhao, L. L.; Schatz, G. C. *J. Phys. Chem.* **2003**, *107*, 668.
(25) Ohno, T.; Bain, J. A.; Schlesinger, T. E. *J. Appl. Phys.* **2007**, *101*, No. 083107.
(26) Rechberger, W.; Hohenau, A.; Leitner, A.; Krenn, J. R.; Lamprecht, B.; Aussenegg, F. R. *Opt. Commun.* **2003**, *220*, 137.
(27) Rill, M. S.; Plet, C.; Thiel, M.; Staude, I.; von Freymann, G.; Linden, S.; Wegener, M. *Nat. Mater.* **2008**, *7*, 543.
(28) Haynes, C. L.; Van Duyne, R. P. *J. Phys. Chem. B* **2001**, *105*, 5599.
(29) Malinsky, M. D.; Kelly, K. L.; Schatz, G. C.; Van Duyne, R. P. *J. Phys. Chem. B* **2001**, *105*, 2343.
(30) Henzie, J.; Lee, M. H.; Odom, T. W. *Nat. Nanotechnol.* **2007**, *2*, 549.
(31) Xue, M.; Yang, Y.; Cao, T. *Adv. Mater.* **2008**, *20*, 596.
(32) Zhang, Y.; Reed, J. C.; Yang, S. *ACS Nano* **2009**, *3*, 2412.
(33) Xu, Q.; Bao, J.; Capasso, F.; Whitesides, G. M. *Angew. Chem., Int. Ed.* **2006**, *45*, 3631.
(34) Xu, Q.; Perez-Castillejos, R.; Li, Z.; Whitesides, G. M. *Nano Lett.* **2006**, *6*, 2163.
(35) Xu, Q.; Bao, J.; Rioux, R. M.; Perez-Castillejos, R.; Capasso, F.; Whitesides, G. M. *Nano Lett.* **2007**, *7*, 2800.
(36) Kim, E.; Xia, Y.; Whitesides, G. M. *J. Am. Chem. Soc.* **1996**, *118*, 5722.
(37) Kim, E.; Whitesides, G. M. *J. Phys. Chem. B* **1997**, *101*, 855.
(38) Viswanathan, N. K.; Kim, D. Y.; Bian, S.; Williams, J.; Liu, W.; Li, L.; Samuelson, L.; Kumar, J.; Tripathy, K. *J. Mater. Chem.* **1999**, *9*, 1941.

DOI: 10.1021/nl903570c | *Nano Lett.* **2010,** *10,* 296-304

(39) Lee, S.; Jeong, Y.-C.; Park, J.-K. *Opt. Express* **2007**, *15*, 14550.
(40) Lee, S.; Jeong, Y.-C.; Park, J.-K. *Appl. Phys. Lett.* **2008**, *93*, No. 031912/1.
(41) Hubert, C.; Fiorini-Debuisschert, C.; Maurin, I.; Nunzi, J.-M.; Raimond, P. *Adv. Mater.* **2002**, *14*, 729.
(42) Juan, M. L.; Plain, J.; Bachelot, R.; Royer, P.; Gray, S. K.; Wiederrecht, G. P. *ACS Nano* **2009**, *3*, 1573.
(43) Xia, Y.; Whitesides, G. M. *Langmuir* **1997**, *13*, 2059.
(44) Friedman, R. S.; McAlpine, M. C.; Ricketts, D. S.; Ham, D.; Lieber, C. M. *Nature* **2005**, *434*, 1085.
(45) Zhang, X.; Sun, B.; Hodgkiss, J. M.; Friend, R. H. *Adv. Mater.* **2008**, *20*, 4455.
(46) Fan, S.; Villeneuve, P. R.; Joannopoulos, J. D. *Phys. Rev. B* **1996**, *54*, 11245.
(47) Yee, K. S. *IEEE Trans. Antennas Propag.* **1966**, *AP-14*, 302.
(48) Berenger, J. *J. Comput. Phys.* **1994**, *114*, 185.

DOI: 10.1021/nl903570c | *Nano Lett.* **2010,** *10,* 296-304